Cellular/Molecular

Activity Induces Fmr1-Sensitive Synaptic Capture of Anterograde Circulating Neuropeptide Vesicles

Samantha L. Cavolo,[1]* Dinara Bulgari,[1]* David L. Deitcher,[2] and Edwin S. Levitan[1]

[1]Department of Pharmacology and Chemical Biology, University of Pittsburgh, Pittsburgh, Pennsylvania 15261, and [2]Department of Neurobiology and Behavior, Cornell University, Ithaca, New York 14853

Synaptic neuropeptide and neurotrophin stores are maintained by constitutive bidirectional capture of dense-core vesicles (DCVs) as they circulate in and out of the nerve terminal. Activity increases DCV capture to rapidly replenish synaptic neuropeptide stores following release. However, it is not known whether this is due to enhanced bidirectional capture. Here experiments at the *Drosophila* neuromuscular junction, where DCVs contain neuropeptides and a bone morphogenic protein, show that activity-dependent replenishment of synaptic neuropeptides following release is evident after inhibiting the retrograde transport with the dynactin disruptor mycalolide B or photobleaching DCVs entering a synaptic bouton by retrograde transport. In contrast, photobleaching anterograde transport vesicles entering a bouton inhibits neuropeptide replenishment after activity. Furthermore, tracking of individual DCVs moving through boutons shows that activity selectively increases capture of DCVs undergoing anterograde transport. Finally, upregulating fragile X mental retardation 1 protein (Fmr1, also called FMRP) acts independently of futsch/MAP-1B to abolish activity-dependent, but not constitutive, capture. Fmr1 also reduces presynaptic neuropeptide stores without affecting activity-independent delivery and evoked release. Therefore, presynaptic motoneuron neuropeptide storage is increased by a vesicle capture mechanism that is distinguished from constitutive bidirectional capture by activity dependence, anterograde selectivity, and Fmr1 sensitivity. These results show that activity recruits a separate mechanism than used at rest to stimulate additional synaptic capture of DCVs for future release of neuropeptides and neurotrophins.

Key words: **axonal transport; peptidergic transmission; secretory granule; SPAIM; synaptic capture**

Significance Statement

Synaptic release of neuropeptides and neurotrophins depends on presynaptic accumulation of dense-core vesicles (DCVs). At rest, DCVs are captured bidirectionally as they circulate through *Drosophila* motoneuron terminals by anterograde and retrograde transport. Here we show that activity stimulates further synaptic capture that is distinguished from basal capture by its selectivity for anterograde DCVs and its inhibition by overexpression of the fragile X retardation protein Fmr1. Fmr1 dramatically lowers DCV numbers in synaptic boutons. Therefore, activity-dependent anterograde capture is a major determinant of presynaptic peptide stores.

Introduction

Synapses are supplied by anterograde axonal transport from the soma, the site of synthesis of synaptic vesicle proteins and dense-core vesicles (DCVs) that contain neuropeptides and neurotrophins. Delivery to synapses was thought to be based on a one-way anterograde trip until it was discovered that DCVs are subject to sporadic capture while traveling bidirectionally through *en passant* boutons as part of long-distance vesicle circulation (Wong et al., 2012). Interestingly, constitutive DCV capture occurs both during fast anterograde and retrograde transport, which are mediated by different motors (i.e., the kinesin 3 family member unc-104/Kif1A and the dynein/dynactin complex, respectively; Jacob and Kaplan, 2003; Pack-Chung et al., 2007; Barkus et al., 2008; Lloyd et al., 2012; Wong et al., 2012). Balanced capture in both directions is advantageous because DCVs are distributed equally among *en passant* boutons (Wong et al., 2012). In principle, bidirectional capture could occur by parallel regulation of anterograde and retrograde motors or by modification of the microtubules that both anterograde and retrograde DCV motors travel on.

Received July 11, 2016; revised Sept. 22, 2016; accepted Sept. 26, 2016.

Author contributions: S.L.C., D.B., and E.S.L. designed research; S.L.C. and D.B. performed research; D.L.D. contributed unpublished reagents/analytic tools; S.L.C., D.B., and E.S.L. analyzed data; E.S.L. wrote the paper.

This work was supported by National Institutes of Health Grant R01NS032385 to E.S.L. We thank Dr. Tanja Godenschwege (Florida Atlantic University) for providing the ShakingB-GAL4 flies.

*S.L.C. and D.B. contributed equally to this work.

The authors declare no competing financial interests.

Correspondence should be addressed to Edwin S. Levitan at the above address. E-mail: elevitan@pitt.edu.

S. L. Cavolo's present address: Allegheny Health Network, 320 East North Avenue, Suite 205 Cancer Institute, Pittsburgh, PA 15212.

DOI:10.1523/JNEUROSCI.2212-16.2016

 0270-6474/16/3611781-07$15.00/0

Before the discovery of bidirectional capture of circulating vesicles, activity was shown to replenish the presynaptic neuropeptide pool following release by inducing Ca^{2+}-dependent capture of DCVs being transported through boutons (Shakiryanova et al., 2006). This result and subsequent experiments (Bulgari et al., 2014) established that capture, rather than delivery or DCV turnover, limits synaptic neuropeptide stores. Activity-dependent capture was first described with a GFP-tagged neuropeptide in the *Drosophila* neuromuscular junction (NMJ), but also occurs with neurotrypsin, wnt/wingless, and brain-derived neurotrophic factor (Ataman et al., 2008; Frischknecht et al., 2008; Dean et al., 2009). Mechanistically, activity-dependent capture was characterized in terms of the rebound in presynaptic GFP-tagged peptide content following release and correlated with decreased retrograde transport (Shakiryanova et al., 2006). However, it is now evident that the reduction in retrograde flux could be caused by enhanced bidirectional capture as DCVs travel back and forth through the terminal as part of vesicle circulation (Wong et al., 2012). Therefore, prior studies support the hypothesis that there is only one synaptic capture mechanism, which is bidirectional and facilitated by activity.

Here we test the above hypothesis by investigating the directionality of activity-dependent capture. Experiments were performed with multiple approaches, including inhibiting retrograde transport, particle tracking, and simultaneous photobleaching and imaging (SPAIM; Wong et al., 2012). Furthermore, the effect of fragile X retardation protein (Fmr1, also called FMRP) was examined because it is known to affect bouton size (Zhang et al., 2001) and neuropeptide release (Annangudi et al., 2010; Francis et al., 2014). Together, these studies establish that different mechanisms mediate synaptic capture at rest and in response to activity.

Materials and Methods

Time lapse, fluorescence recovery after photobleaching (FRAP), and SPAIM experiments were performed at the *Drosophila* NMJ in accordance with previously published methods (Levitan et al., 2007; Wong et al., 2012, 2015; Cavolo et al., 2015). Third-instar *Drosophila* of either sex used for imaging were OK6>Dilp2-GFP/CyO and ShB (ShakingB)>Anf-GFP flies. The UAS constructs were generated by us (Rao et al., 2001; Wong et al., 2012), OK6-GAL4 was obtained from the Bloomington *Drosophila* Stock Center, and ShB-GAL4 flies were kindly provided by Dr. Tanja Godenschwege (Florida Atlantic University). Third-instar larvae were filleted in HL3 saline, which contains (in mM) the following: 70 NaCl, 5 KCl, 1.5 $CaCl_2$, 20 $MgCl_2$, 10 $NaHCO_3$, 5 trehalose, 115 sucrose, and 5 sodium HEPES, pH 7.2, or HL3 saline in which Ca^{2+} was replaced with 0.5 mM EGTA (0 Ca^{2+} HL3). Larvae were viewed with Olympus objectives (60×; 1.1 or 1.0 numerical aperture) on a Fluoview 1000 scanning confocal microscope (Figs. 1–4*C*, 5*B*), an Olympus microscope equipped with a Yokogawa spinning disk confocal module and a Hamamatsu EMCCD camera set up by the Solamere Technology Group (Figs. 4*D*,*E*, 5*A*; see 7*B*), or an Olympus wide-field microscope (Figs. 6, 7*A*). SPAIM (Wong et al., 2012) experiments were performed on a Fluoview microscope equipped with two scanners. As described in the results, in SPAIM experiments one scanner positioned a beam to photobleach either DCVs moving by anterograde or retrograde transport into a bouton, while the second scanner imaged the bouton in the region of interest (ROI). Nerve stimulation (70 Hz) was performed in HL3 supplemented with 10 mM glutamate to prevent muscle contraction. For labeling small synaptic vesicles, fillets were depolarized for 3 min in saline in which 70 mM Na^+ was substituted with K^+ in the presence of 4 μM FM4-64. To label mitochondria, fillets were incubated for 5 min in 100 μM MitoTracker Red chloromethyl-X-rosamine (MitoTracker Red) in 0 Ca^{2+} saline. In both cases, the dyes, which were purchased from Invitrogen, were washed out of the bath and labeled organelles were imaged by confocal microscopy. Imaging data were analyzed in ImageJ (RRID: SCR_003070), while graphing and statistics were performed with Graphpad Prism (RRID:SCR_002798). When there were only two experimental conditions, data were analyzed with unpaired or, when possible, paired *t* tests. When there were >2 experimental conditions, data were analyzed by one-way ANOVA and Dunnett's post-test. For Figures 1 and 2, data during the recovery phase were fit by linear regression and the significance of changes in slope was determined. For all statistical tests, two-tailed *p* values were set with 0.05 set as the threshold for statistical significance.

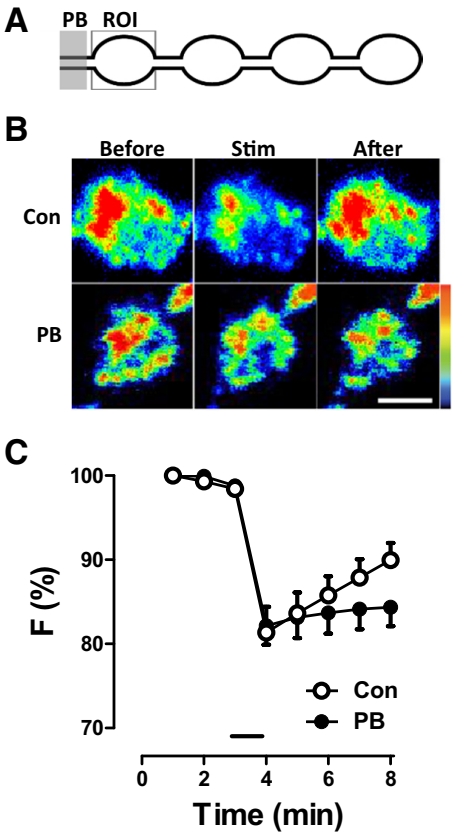

Figure 1. Anterograde DCVs contribute to activity-dependent capture. ***A***, Design of SPAIM experiment to detect contribution of anterograde DCVs. The axon was continuously photobleached (PB) while the most proximal bouton in the ROI was imaged. ***B***, Pseudocolor images from a single experiment showing neuropeptide content before, immediately after 1 min of 70 Hz stimulation (Stim), and 4 min later. Scale bar, 2 μm. ***C***, Quantification of the effect of upstream PB on stimulation responses. Bar indicates 70 Hz stimulation. For both controls (Con) and PB experiments, $n = 5$.

Results

Anterograde vesicles contribute to activity-dependent capture

To determine the contribution of anterograde transport to activity-dependent capture of DCVs, a photobleaching beam was positioned in the axon upstream of the most proximal bouton in an NMJ terminal branch (Fig. 1*A*). Thus, DCVs containing GFP-tagged *Drosophila* insulin-like peptide 2 (Dilp2; Wong et al., 2012) traveling by anterograde transport on their way to enter the most proximal unbleached bouton were photobleached while DCVs undergoing retrograde transport and residing boutons were unaffected. Then while simultaneously photobleaching the axon and imaging the proximal bouton in the ROI, the axon was stimulated at 70 Hz to evoke release. Under these conditions, activity evokes initial decreases in DCV/neuropeptide fluorescence in both photobleached and unbleached control animals that are statistically indistinguishable (Fig. 1*B*,*C*; unpaired *t* test). Prior studies with biochemical assays, accumulation of fluores-

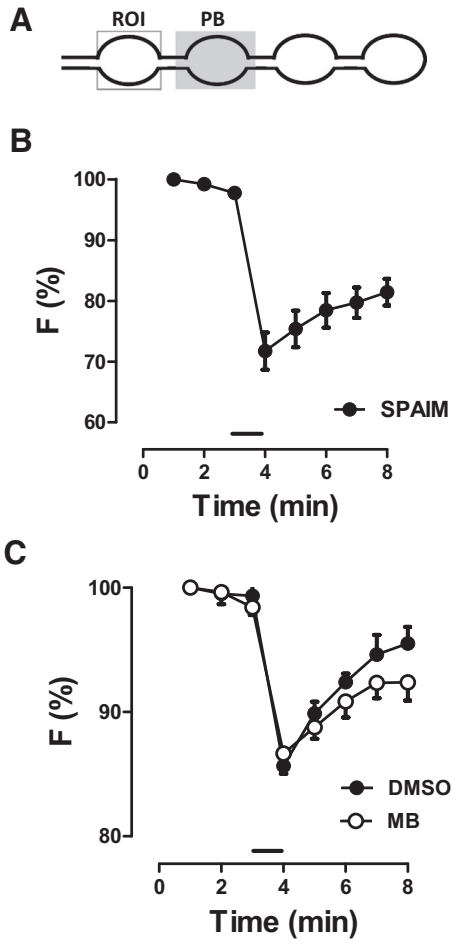

Figure 2. Activity-dependent capture does not require retrograde DCVs. ***A***, Design of SPAIM experiments to detect contribution of retrograde DCVs. ***B***, Release and rebound due to capture are evident with continuous downstream photobleaching. $n = 7$. ***C***, Release and capture persist after inhibiting retrograde transport with MB. DMSO control, $n = 5$; MB, $n = 6$. Bars, 70 Hz stimulation.

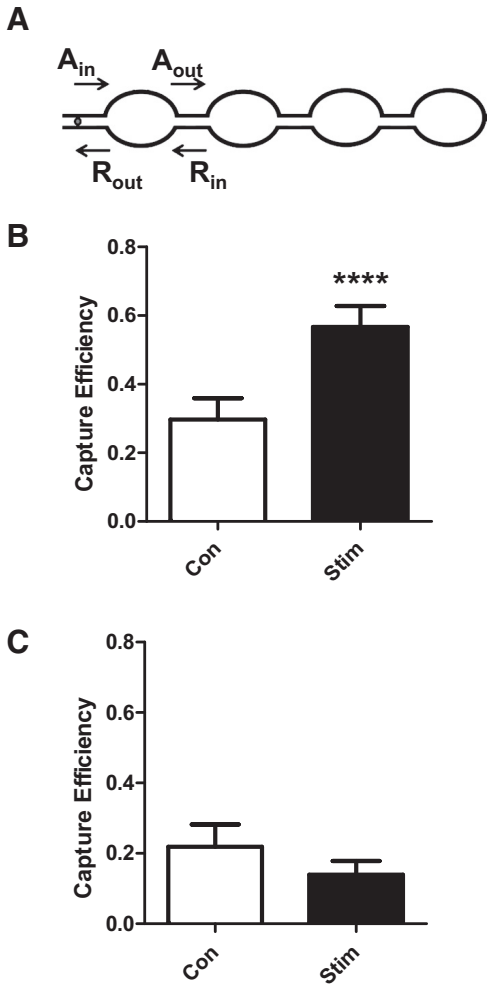

Figure 3. Activity selectively increases capture of anterograde DCVs. ***A***, DCV flux was measured in and out of the most proximal bouton in a branch following its photobleaching. Anterograde capture efficiency was calculated as $(A_{in} - A_{out})/A_{in}$, while retrograde capture equaled $(R_{in} - R_{out})/R_{in}$. ***B***, Effect of stimulation (Stim) on anterograde capture efficiency ($n = 13$, $p < 0.0001$, paired t test). ***C***, Effect of stimulation on retrograde capture efficiency ($n = 13$). Paired t test showed that there was no significant change.

cence in other tissues, loss of immunofluorescence, Ca^{2+} dependence, and sensitivity to N-ethylmaleimide [a defining feature of SNARE (soluble N-ethylmaleimide-sensitive factor activating protein receptor)-dependent exocytosis] have established that this loss of GFP-tagged neuropeptide is produced by release (Burke et al., 1997; Rao et al., 2001; Husain and Ewer, 2004; Shakiryanova et al., 2005; Loveall and Deitcher, 2010). Furthermore, the use of a pH-resistant GFP and the low acidity of vesicles in this preparation (Sturman et al., 2006) exclude a role for pH in these responses. Following release, there is replacement of released presynaptic neuropeptide (i.e., the postrelease rebound in neuropeptide content), which inhibiting DCV transport and measuring DCV flux showed is mediated by capture of circulating DCVs that constantly flow through NMJ boutons (Shakiryanova et al., 2006; Wong et al., 2012). Notably, this recovery phase was reduced with upstream photobleaching in axons (Fig. 1*B*,*C*; $n = 5$ for each condition).

Three types of analysis showed that this effect was statistically significant. In each case, we took into account that another experimental condition, the effect of downstream photobleaching of retrograde DCVs (see below; Fig. 2*A*,*B*), would require multiple-comparison tests. First, the recovery of fluorescence following stimulation differed based on one-way ANOVA followed by Dunnett's post-test ($p < 0.05$). Second, to take into account variation in release, fractional recovery was calculated and found to differ with one-way ANOVA followed by Dunnett's post-test ($p < 0.001$). Finally, linear regression analysis of the plots during the recovery phase showed that the slope was significantly affected by axonal photobleaching ($p < 0.001$). Therefore, three statistical analyses showed that photobleaching anterograde DCVs significantly reduced activity-dependent capture. This result provides independent verification of the conclusion by Shakiryanova et al. (2006) that the recovery of neuropeptide stores following release cannot be attributed to a change in turnover or exit of resident DCVs, but instead requires DCV axonal transport. Therefore, we focused on whether capture is bidirectional.

Activity-dependent capture without retrograde transport

With vesicle circulation between the axon initial segment and nerve terminals, anterograde DCVs contribute to retrograde flux of DCVs through boutons. Therefore, given the requirement for anterograde axonal transport demonstrated above, we sought to determine the impact of retrograde transport on activity-dependent DCV capture. Specifically, replenishment of presynaptic neuropeptide in the minutes following activity-evoked

release was again studied at the *Drosophila* NMJ, but in this case the photobleaching beam was positioned just downstream of the most proximal bouton in a nerve terminal branch while simultaneously imaging neuropeptide content (Fig. 2*A*). Continuous photobleaching ensured that any DCVs traveling in the retrograde direction into the imaged bouton were photobleached and therefore unable to contribute to the replacement of released presynaptic neuropeptide from the bouton in the ROI. Despite increased release (i.e., the immediate drop in Dilp2-GFP fluorescence) that might reflect local depolarization, the recovery of presynaptic neuropeptide stores indicative of activity-dependent capture of DCVs was still evident (Fig. 2*B*). Indeed, using the analysis described above, there was no statistically significant effect of photobleaching retrograde vesicles on the extent of recovery, the fractional recovery or the linear regression slopes for data between 4 and 8 min. Therefore, eliminating the contribution of DCVs undergoing retrograde transport into the bouton of interest with photobleaching did not abolish activity-dependent capture.

To independently test this conclusion without an accompanying change in release or any photobleaching, retrograde transport was inhibited with the dynactin/F-actin disruptor mycalolide B (MB; Cavolo et al., 2015). Specifically, MB was applied at 2 μM for 20 min, which eliminates retrograde transport in the axon and terminal while preserving anterograde DCV transport (Cavolo et al., 2015). Strikingly, activity-evoked release was unaffected and the subsequent rebound in presynaptic neuropeptide content (i.e., the slow recovery in fluorescence) indicative of capture was still evident in the presence of MB (Fig. 2*C*). Again, statistical analysis of extent of recovery, fractional recovery, and linear regression slopes showed that there is no significant change in the recovery phase. These results show that activity-evoked kiss-and-run exocytic release from presynaptic DCVs (Wong et al., 2015) and activity-dependent capture are independent of F-actin and retrograde transport, which are both targeted by MB. Thus, MB verified that activity-dependent capture does not require retrograde DCV transport. Together, the above experiments show that activity-dependent capture relies selectively on anterograde transport of DCVs to the bouton.

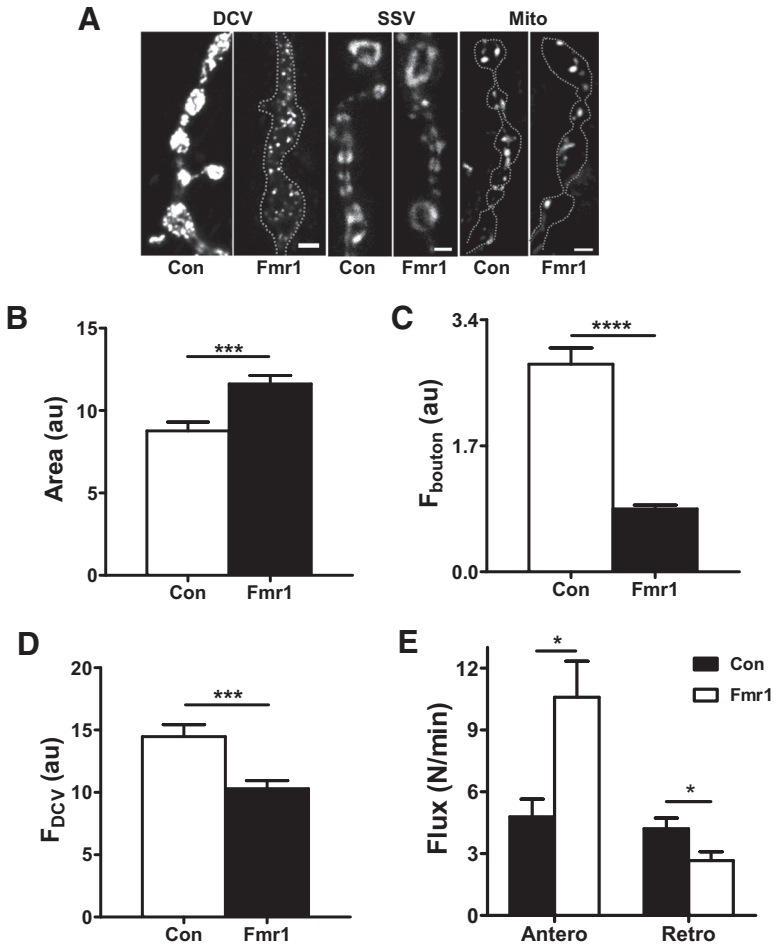

Figure 4. Fmr1 effects on type-Ib boutons and DCVs. ***A***, Images showing Control (Con) and Fmr1 overexpressing type-Ib boutons with DCVs labeled with Dilp2-GFP (left), SSVs labeled with FM4-64 (center), and mitochondria (Mito) labeled with MitoTracker Red (right). Dashed lines show outline of boutons. Scale bars, 2 μm. ***B***, Fmr1 increases bouton area. Con, $n = 59$; Fmr1, $n = 73$. ***C***, Fmr1 decreases total Dilp2-GFP fluorescence per bouton (F_{bouton}) measured in confocal image stacks. Con, $n = 59$; Fmr1, $n = 73$. ***D***, Fmr1 decreases individual DCV fluorescence (F_{DCV}). Con, $n = 138$; Fmr1, $n = 114$. ***E***, Effect of Fmr1 on DCV flux through proximal boutons. Con, $n = 8$; Fmr1, $n = 9$. $^*p < 0.05$; $^{***}p < 0.001$, $^{****}p < 0.0001$, unpaired *t* test.

Capture efficiency for anterograde and retrograde DCVs

To directly quantify the contributions of anterograde and retrograde capture without the confound of release, fractional capture efficiency was measured based on single particle tracking through photobleached boutons. These experiments were initially performed with type-Ib boutons, but later type-Is boutons were used because they displayed activity-dependent capture (see below), had DCV flux in both directions comparable to that of type-Ib boutons (2–3 per minute), and presented two technical advantages: (1) single DCVs were ~2-fold brighter and so yielded better signal-to-noise ratios, and (2) the smaller size of these boutons ensured that mobile DCVs stayed in focus (i.e., the bouton was fully contained in the confocal depth of field). Therefore, a proximal Is bouton was photobleached and time-lapse imaging was used to follow DCVs entering and leaving the bouton by anterograde and retrograde transport (Fig. 3*A*). Finally, to avoid the contributions of upstream and/or downstream capture to flux (see Introduction), capture efficiency was quantified in single photobleached proximal boutons as the fractional difference in entering and leaving DCVs for each direction (i.e., for anterograde DCVs: $(A_{in} - A_{out})/A_{in}$; for retrograde DCVs: $(R_{in} - R_{out})/R_{in}$; Fig. 3*A*) in the 3 min periods before and after 70 Hz stimulation for 1 min. This type of quantification previously demonstrated differences in DCV capture efficiency in type-Ib and type-III boutons (Wong et al., 2012; Bulgari et al., 2014). As expected, before stimulation (i.e., at rest) DCV capture in type-Is boutons occurred in both directions with low efficiency (Fig. 3*B*,*C*, open bars). However, following stimulation, capture efficiency was increased for DCVs undergoing anterograde transport (Fig. 3*B*; $n = 13$ boutons, $p < 0.0001$, paired *t* test). In contrast, capture efficiency for retrograde DCVs in these same boutons did not change significantly in response to activity (Fig. 3*C*). Also, the

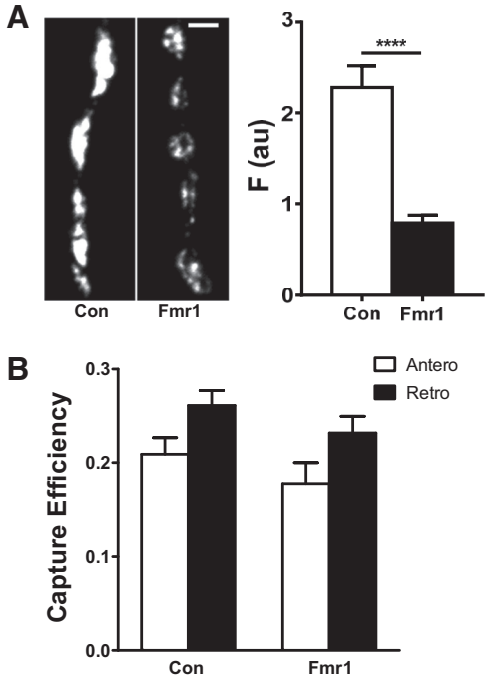

Figure 5. Fmr1 overexpression does not alter constitutive capture efficiency in type-Is boutons. ***A***, Left, Representative images of type-Is boutons in control (Con) and Fmr1-overexpressing NMJs. Right, Quantification of bouton fluorescence. Con, $n = 44$; Fmr1, $n = 40$. ****$p < 0.0001$, unpaired t test. ***B***, Capture efficiency measurements were made as in Figure 3. Con, $n = 9$; Fmr1, $n = 12$.

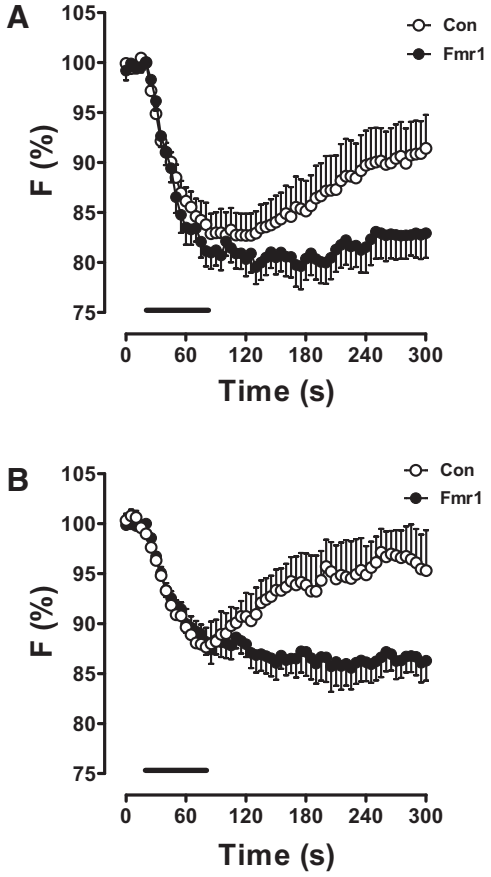

Figure 6. Fmr1 overexpression inhibits activity-dependent capture. ***A***, Data from type-Is boutons. Control (Con), $n = 6$; Fmr1, $n = 8$. ***B***, Data from type-Ib boutons. Con, $n = 4$; Fmr1, $n = 10$. Bars, 70 Hz stimulation.

effect on anterograde transport became statistically insignificant in the absence of extracellular Ca^{2+} ($n = 8$) and was not associated with DCVs changing direction. Therefore, activity-induced Ca^{2+}-dependent capture is not bidirectional. Rather, the optical and pharmacological perturbations in Figures 1 and 2 and the particle tracking in Figure 3 all show that activity selectively increases capture of DCVs undergoing anterograde transport.

Fmr1 overexpression selectively inhibits activity-dependent capture of DCVs

Fmr1, the fragile X retardation 1 protein, increases the size of type-Ib boutons at the *Drosophila* NMJ (Zhang et al., 2001). Therefore, to examine the contribution of DCV transport and capture to the Fmr1 effect, neuropeptide accumulation and DCV traffic were studied. Unfortunately, animals expressing a GFP-tagged neuropeptide and two *Fmr1* mutants (Delta50M and Delta113M) did not survive to the third-instar developmental stage. Therefore, our experiments focused on the effects of Fmr1 overexpression. As expected, type-Ib boutons were enlarged with Fmr1 overexpression in motoneurons (Fig. 4*A*,*B*; $p < 0.001$). However, neuropeptide intensity per bouton (F_{bouton}) measured in confocal stacks was dramatically attenuated to only 30% of controls ($p < 0.0001$), showing that neuropeptide stores do not scale with bouton enlargement (Fig. 4*A*,*C*). In contrast, labeling of small synaptic vesicles (SSVs) with the styryl dye FM4-64 did not reveal an effect of Fmr1 on the abundance of SSVs in boutons (Fig. 4*A*); quantification of normalized FM4-64 fluorescence was $100 \pm 4.7\%$ ($n = 13$) for controls and $97.3 \pm 7.0\%$ ($n = 12$) with Fmr1. Likewise, there was no obvious difference for mitochondria labeled with MitoTracker Red in boutons (Fig. 4*A*). Thus, the Fmr1 effect is selective for DCVs.

Analysis of individual DCVs undergoing transport in the terminal revealed that with Fmr1 overexpression, individual DCVs contained 71% of the peptide in control DCVs (Fig. 4*D*; $p < 0.001$), but arrived more frequently by anterograde flux (i.e., at more than twice the rate), while retrograde transport decreased (Fig. 4*E*; $p < 0.05$). Taking all of these measurements together revealed that total neuropeptide delivery [i.e., total (anterograde plus retrograde) flux into the bouton multiplied by individual DCV content] was essentially unchanged. Yet, total neuropeptide content (Fig. 4*C*) and DCV numbers per bouton (derived by dividing total peptide fluorescence by individual DCV fluorescence) were reduced >2-fold despite an increase in bouton size (Fig. 4*B*). Therefore, as neuropeptide content per DCV (Fig. 4*D*, F_{DCV}) cannot account for this effect, Fmr1 must either increase release or inhibit DCV capture to reduce the steady-state presynaptic DCV number.

To determine the effect of Fmr1 overexpression on constitutive capture, capture efficiency was quantified in 0 Ca^{2+}. Importantly, the reduction in peptide content induced by Fmr1 overexpression in type-Ib boutons (Fig. 4*A*,*C*) was also evident in type-Is boutons (Fig. 5*A*). Furthermore, flux analysis in type-Is boutons showed that constitutive bidirectional capture was maintained as both anterograde and retrograde capture efficiencies were unaffected by Fmr1 (Fig. 5*B*). Therefore, the drop in neuropeptide content must arise from regulating either release or capture induced by activity.

To distinguish between these two hypotheses, we assessed the impact of activity in type-Ib boutons on muscle 4 and in type-Is boutons on muscle 6/7. In both cases, Fmr1 overexpression did not markedly affect synaptic neuropeptide release. However, at

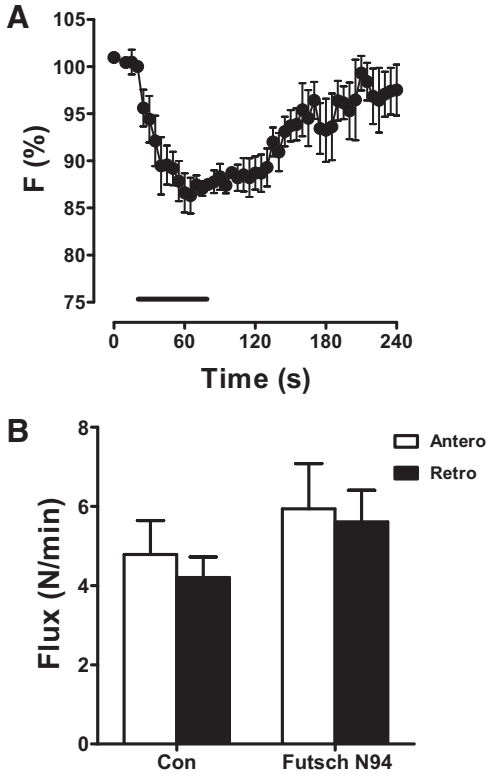

Figure 7. Futsch/Map1B does not affect activity-dependent DCV capture or flux. ***A***, Macroscopic release and capture responses to stimulation of type-Ib boutons in the *Futsch N94* mutant. Bar, 70 Hz stimulation. ***B***, DCV flux is unaffected in Futsch N94 boutons. Control (Con), $n = 8$; *Futsch N94*, $n = 6$.

both synapses activity-dependent capture was abolished (Fig. 6*A*,*B*). Therefore, the effect of a genetic perturbation on activity-dependent, but not constitutive, capture and directional selectivity shows that activity induces a distinct capture mechanism. Furthermore, the decrease in neuropeptide/DCV content accompanying the selective inhibition of activity-dependent capture induced by Fmr1 shows that that activity-dependent capture contributes to steady-state presynaptic peptide stores.

The effect of Fmr1 on Ib bouton size is linked to futsch/MAP1B; for example, the N94 *futsch* mutant mimics the effect of Fmr1 overexpression (Roos et al., 2000; Zhang et al., 2001). However, this mutant displayed normal presynaptic neuropeptide stores, activity-dependent release and capture, and DCV flux (Fig. 7). Therefore, the inhibition of activity-dependent anterograde capture by Fmr1 must be through a *futsch*-independent mechanism.

Discussion

Until recently, it was thought that presynaptic neuropeptide stores were set by controlling synthesis and delivery by fast one-way axonal transport of DCVs. However, studies of the *Drosophila* NMJ have shown that there is an excess of DCVs delivered to type-I boutons by long-distance vesicle circulation. Therefore, because DCV delivery is not limiting, the presynaptic neuropeptide pool is determined by capture, which was found to be bidirectional (Wong et al., 2012). However, in addition to constitutive capture, activity induces Ca^{2+}-dependent capture (Shakiryanova et al., 2006). This is advantageous because tapping into the circulating vesicle pool removes delays associated with synthesis and transport, which can take days in humans, to rapidly replace released peptides. Surprisingly, experiments presented here demonstrate that activity-dependent capture is unidirectional and selectively sensitive to a genetic perturbation (i.e., Fmr1 overexpression). Therefore, activity does not simply enhance constitutive bidirectional capture that operates at rest, but instead stimulates an independent synaptic capture mechanism.

Previously, it was not possible to genetically block activity-dependent capture to determine its contribution to steady-state presynaptic stores. However, this study documented inhibition of activity-dependent capture by Fmr1 overexpression. As this was accompanied by a dramatic decrease in presynaptic DCV number, we conclude that activity-dependent capture makes a large contribution to steady-state presynaptic peptide stores and hence the capacity for future release. At the *Drosophila* NMJ, DCVs contain a bone morphogenic protein and neuropeptides (Anderson et al., 1988; James et al., 2014). Thus, it is possible that activity-dependent capture affects development and acute synaptic function.

Capture efficiency measurements revealed that the previously detected decrease in retrograde traffic following activity was an indirect effect of vesicle circulation; activity-induced capture of only anterograde DCVs at each *en passant* bouton simply leaves fewer DCVs for the retrograde trip back into the axon without changing retrograde capture. Of interest, anterograde selectivity for activity-induced capture rules out mechanisms that would perturb transport in both directions (e.g., microtubule breaks). DCV anterograde transport is mediated by the unc-104/Kif1A motor, which also transports SSV proteins and is required for formation of boutons (Hall and Hedgecock, 1991; Jacob and Kaplan, 2003; Pack-Chung et al., 2007; Barkus et al., 2008). Therefore, activity-dependent capture may regulate unc-104/Kif1A to affect synaptic release of both small-molecule transmitters and peptides. However, alternative targets could be involved, including proteins that mediate DCV interaction with this anterograde motor or alter the DCV itself (e.g., its phosphoinositides, which may bind to the unc-104/Kif1A pleckstrin homology domain; Klopfenstein and Vale, 2004).

Further insights regarding Fmr1 and DCVs

The hypothesis that increased DCV capture contributes to the larger boutons produced by Fmr1 overexpression led us to study the effects of Fmr1 on constitutive and activity-dependent capture of DCVs. However, activity-dependent capture was inhibited and constitutive bidirectional capture was unaffected. Also, futsch/Map1B, which is linked to bouton enlargement (Zhang et al., 2001), did not affect activity-dependent DCV capture. Therefore, DCV capture must not account for Fmr1-induced bouton enlargement.

In addition to DCV capture results, these experiments revealed that Fmr1 overexpression decreased the content of individual DCVs and simultaneously increased DCV flux to preserve delivery to terminals. At this point we cannot distinguish whether this homeostatic control of neuropeptide delivery to terminals occurs because greater DCV biogenesis results in less efficient neuropeptide packaging or because less efficient packaging stimulates compensatory DCV biogenesis and delivery. Alternatively, the apparent homeostatic effect could be a coincidental consequence of separate Fmr1 effects on DCV content and transport. In any case, to our knowledge, such apparent homeostasis between DCV content and flux into terminals has not been described previously.

Fmr1 is known to bind to channels and to regulate the expression of many genes (Ferron, 2016). Because release evoked by action potentials was normal, it is unlikely that channel effects

account for the effects of Fmr1 overexpression on content, flux, and capture of DCVs. As noted above, we examined the role of futsch/Map1B, which is downregulated by Fmr1 overexpression and participates in the effect on bouton size (Zhang et al., 2001), but experiments with a mutant showed that futsch/Map1B is not involved in the DCV effects documented here. Therefore, in the future it will be of interest to identify the Fmr1 target that accounts for the effect on activity-dependent synaptic capture of anterograde DCVs. It will then be possible to determine whether this target is related to Fmr1 effects on neuropeptide release and neuropeptide-dependent behaviors (Annangudi et al., 2010; Francis et al., 2014).

References

Anderson MS, Halpern ME, Keshishian H (1988) Identification of the neuropeptide transmitter proctolin in *Drosophila* larvae: characterization of muscle fiber-specific neuromuscular endings. J Neurosci 8:242–255. Medline

Annangudi SP, Luszpak AE, Kim SH, Ren S, Hatcher NG, Weiler IJ, Thornley KT, Kile BM, Wightman RM, Greenough WT, Sweedler JV (2010) Neuropeptide release is impaired in a mouse model of fragile X mental retardation syndrome. ACS Chem Neurosci 1:306–314. CrossRef Medline

Ataman B, Ashley J, Gorczyca M, Ramachandran P, Fouquet W, Sigrist SJ, Budnik V (2008) Rapid activity-dependent modifications in synaptic structure and function require bidirectional Wnt signaling. Neuron 57:705–718. CrossRef Medline

Barkus RV, Klyachko O, Horiuchi D, Dickson BJ, Saxton WM (2008) Identification of an axonal kinesin-3 motor for fast anterograde vesicle transport that facilitates retrograde transport of neuropeptides. Mol Biol Cell 19:274–283. CrossRef Medline

Bulgari D, Zhou C, Hewes RS, Deitcher DL, Levitan ES (2014) Vesicle capture, not delivery, scales up neuropeptide storage in neuroendocrine terminals. Proc Natl Acad Sci U S A 111:3597–3601. CrossRef Medline

Burke NV, Han W, Li D, Takimoto K, Watkins SC, Levitan ES (1997) Neuronal peptide release is limited by secretory granule mobility. Neuron 19:1095–1102. CrossRef Medline

Cavolo SL, Zhou C, Ketcham SA, Suzuki MM, Ukalovic K, Silverman MA, Schroer TA, Levitan ES (2015) Mycalolide B dissociates dynactin and abolishes retrograde axonal transport of dense-core vesicles. Mol Biol Cell 26:2664–2672. CrossRef Medline

Dean C, Liu H, Dunning FM, Chang PY, Jackson MB, Chapman ER (2009) Synaptotagmin-IV modulates synaptic function and long-term potentiation by regulating BDNF release. Nat Neurosci 12:767–776. CrossRef Medline

Ferron L (2016) Fragile X mental retardation protein controls ion channel expression and activity. J Physiol. Advance online publication. Retrieved Oct. 3, 2016. CrossRef Medline

Francis SM, Sagar A, Levin-Decanini T, Liu W, Carter CS, Jacob S (2014) Oxytocin and vasopressin systems in genetic syndromes and neurodevelopmental disorders. Brain Res 1580:199–218. CrossRef Medline

Frischknecht R, Fejtova A, Viesti M, Stephan A, Sonderegger P (2008) Activity-induced synaptic capture and exocytosis of the neuronal serine protease neurotrypsin. J Neurosci 28:1568–1579. CrossRef Medline

Hall DH, Hedgecock EM (1991) Kinesin-related gene unc-104 is required for axonal transport of synaptic vesicles in C. elegans. Cell 65:837–847. CrossRef Medline

Husain QM, Ewer J (2004) Use of targetable gfp-tagged neuropeptide for visualizing neuropeptide release following execution of a behavior. J Neurobiol 59:181–191. CrossRef Medline

Jacob TC, Kaplan JM (2003) The EGL-21 carboxypeptidase E facilitates acetylcholine release at *Caenorhabditis elegans* neuromuscular junctions. J Neurosci 23:2122–2130. Medline

James RE, Hoover KM, Bulgari D, McLaughlin CN, Wilson CG, Wharton KA, Levitan ES, Broihier HT (2014) Crimpy enables discrimination of presynaptic and postsynaptic pools of a BMP at the Drosophila neuromuscular junction. Dev Cell 31:586–598. CrossRef Medline

Klopfenstein DR, Vale RD (2004) The lipid binding pleckstrin homology domain in UNC-104 kinesin is necessary for synaptic vesicle transport in Caenorhabditis elegans. Mol Biol Cell 15:3729–3739. CrossRef Medline

Levitan ES, Lanni F, Shakiryanova D (2007) In vivo imaging of vesicles and release at the Drosophila neuromuscular junction. Nat Protocols 2:1117–1125. CrossRef Medline

Lloyd TE, Machamer J, O'Hara K, Kim JH, Collins SE, Wong MY, Sahin B, Imlach W, Yang Y, Levitan ES, McCabe BD, Kolodkin AL (2012) The p150(Glued) CAP-Gly domain regulates initiation of retrograde transport at synaptic termini. Neuron 74:344–360. CrossRef Medline

Loveall BJ, Deitcher DL (2010) The essential role of bursicon during *Drosophila* development. BMC Dev Biol 10:92. CrossRef Medline

Pack-Chung E, Kurshan PT, Dickman DK, Schwarz TL (2007) A Drosophila kinesin required for synaptic bouton formation and synaptic vesicle transport. Nat Neurosci 10:980–989. CrossRef Medline

Rao S, Lang C, Levitan ES, Deitcher DL (2001) Visualization of neuropeptide expression, transport, and exocytosis in Drosophila melanogaster. J Neurobiol 49:159–172. CrossRef Medline

Roos J, Hummel T, Ng N, Klämbt C, Davis GW (2000) Drosophila Futsch regulates synaptic microtubule organization and is necessary for synaptic growth. Neuron 26:371–382. CrossRef Medline

Shakiryanova D, Tully A, Hewes RS, Deitcher DL, Levitan ES (2005) Activity-dependent liberation of synaptic neuropeptide vesicles. Nat Neurosci 8:173–178. CrossRef Medline

Shakiryanova D, Tully A, Levitan ES (2006) Activity-dependent synaptic capture of transiting peptidergic vesicles. Nat Neurosci 9:896–900. CrossRef Medline

Sturman DA, Shakiryanova D, Hewes RS, Deitcher DL, Levitan ES (2006) Nearly neutral secretory vesicles in Drosophila nerve terminals. Biophys J 90:L45–L47. CrossRef Medline

Wong MY, Zhou C, Shakiryanova D, Lloyd TE, Deitcher DL, Levitan ES (2012) Neuropeptide delivery to synapses by long range vesicle circulation and sporadic capture. Cell 148:1029–1038. CrossRef Medline

Wong MY, Cavolo SL, Levitan ES (2015) Synaptic neuropeptide release by dynamin-dependent partial release from circulating vesicles. Mol Biol Cell 26:2466–2474. CrossRef Medline

Zhang YQ, Bailey AM, Matthies HJ, Renden RB, Smith MA, Speese SD, Rubin GM, Broadie K (2001) Drosophila fragile X-related gene regulates the MAP1B homolog Futsch to control synaptic structure and function. Cell 107:591–603. CrossRef Medline